

Variable-Performance Electro Spray Maneuvers Optimization

Giuseppe Di Pasquale^{*†§}, David Villegas-Prado^{*}, Manuel Sanjurjo-Rivo[§] and Daniel Pérez Grande^{*}

^{*}*IENAI SPACE - Av. Gregorio Peces Barba, 1, Leganes, 28919, Spain*

[§]*Universidad Carlos III de Madrid - Av. de la Universidad, 30, Leganes, 28919, Spain*

giuseppe.dipasquale@ienai.space · david.villegas@ienai.space

[†]Corresponding author

Abstract

Electrospray propulsion is gaining popularity due to its high efficiency at low power, the use of inert liquid propellants, and near-instantaneous operations. Externally wetted electrospays, in particular, can operate in different emission regimes, which yields different performance points. Real-time dynamic switching between these regimes could enable variable-performance maneuvers, leading to propellant and duration savings. This study focuses on the optimization of variable-performance electro spray maneuvers for small satellites in LEO. The methodology employs a genetic algorithm to select the set point depending on a maneuvering efficiency term, aimed at minimizing multiple objectives. A numerical example demonstrates the benefits of this approach, presenting practical considerations regarding operations.

1. Introduction

Electric Propulsion (EP) is establishing itself as an advantageous alternative to Chemical Propulsion (CP) for space mobility of small satellites, due to the propellant savings deriving from the high exhaust velocities attainable and the consequent large total impulse deliverable in a contained mass and volume [3, 13]. However, unlike chemical propulsion, these systems can only reach limited thrust levels; the acceleration imparted by electrostatic and electromagnetic EP systems is usually well below 0.001 m/s^2 . The long trajectories deriving from such low acceleration magnitudes require optimization routines aimed at reducing the propellant and, most importantly, the duration of the maneuvers. Among the multitude of existing EP technologies, a growing interest is building up around electrospays because of their competitive performance in the low power range, where Hall Effect thrusters or gridded ion engines suffer from efficiency losses and become less appealing. Besides other qualities, such as high efficiency, the use of inert liquid propellants, lack of neutralizer, and short operations transients timescale [16], externally wetted electro spray exhibit different emission regimes depending on the voltage set-point applied [18], which can affect significantly the performance delivered by the system. Two main emission regimes can be individuated: "ionic" and "droplet". These regimes are characterized respectively by high specific impulse and high thrust-to-power ratio. This paper proposes to combine the operation of these regimes, switching dynamically between them throughout the maneuver, aiming at improving the exploitation of the performance of the thruster. This enables trading thrust for specific impulse when most energetically convenient, and vice-versa, which has been demonstrated to lead to improved maneuver performance [12, 7]. Additionally, the high thrust-to-power ratio mode could be exploited for collision avoidance maneuvers, boosting the responsiveness of the satellite.

However, the optimization of a low-thrust variable performance system is complex and requires a robust and effective tool to obtain optimal solutions. Several works employed indirect optimization methods to solve the variable-performance time-fixed minimum-fuel problem, typically for interplanetary applications [9, 1, 8, 11, 2]. A direct method for GTO-GEO transfer including a realistic efficiency model was proposed in [10] and an analytical solution for circular orbits was developed by [17]. Literature shows that variable performance maneuvers can be up to 20% more convenient, although the focus is on single-objective and interplanetary transfers. This work presents the application of a novel methodology for optimizing variable-performance maneuvers based on [7] and applied to a thruster with discrete states. This methodology employs a robust architecture for multi-objective optimization which is applied to a realistic model of an electro spray technology-based system. The goal of the paper is to demonstrate that a variable performance thruster could be used to improve the maneuvering capabilities of small satellites, at the cost of a minor operational complexity increase. The focus of the study is on Low Earth Orbit (LEO) transfers, specifically for constellation operations, including commissioning, station-keeping, and deorbiting.

2. Problem statement

The problem is described as a multi-objective optimal control problem, stated in the following notation:

$$\begin{aligned}
 & \text{minimize} \quad J = [m_p, t_f]^T, \\
 & \text{with respect to} \quad \mathbf{u} \in U \\
 & \text{subject to} \quad \dot{\mathbf{x}}(t) = \mathbf{f}(t, \mathbf{x}(t), \mathbf{u}(t)) \\
 & \quad \mathbf{x}(t_0) - \boldsymbol{\psi}_0 = 0, \\
 & \quad \mathbf{x}(t_f) - \boldsymbol{\psi}_f = 0
 \end{aligned} \tag{1}$$

where \mathbf{x} are the dynamic states, governed by the system of non-linear differential equations \mathbf{f} . The controls \mathbf{u} are bounded to a feasible set U . J is the vectorial objective function, comprising the propellant mass needed to perform the maneuver (m_p) and the final time, namely the maneuver duration (t_f). $\boldsymbol{\psi}_0$ and $\boldsymbol{\psi}_f$ are the boundary conditions at the initial time t_0 and final time t_f , representing the initial and final states of the satellite.

2.1 Dynamics

The dynamics of the problem \mathbf{f} are modeled with a modified equinoctial elements formulation of Gauss Variational Equations:

$$\dot{\mathbf{x}}_m(t) = A(\mathbf{x}_m(t))\mathbf{p}(t) + \mathbf{b}(\mathbf{x}_m(t)), \tag{2}$$

where \mathbf{x}_m is a subset of the state vector (\mathbf{x}), containing the modified equinoctial elements, defined as:

$$\mathbf{x}_m = [p \ f_m \ g_m \ h_m \ k_m \ L]^T, \tag{3}$$

where p is the semi-latus rectum, L the true longitude and f_m , g_m , h_m , and k_m are the remaining elements. The matrix A is written as:

$$A = \sqrt{\frac{p}{\mu}} \begin{bmatrix} 0 & \frac{2p}{w} & 0 \\ \sin L & \frac{1}{w}[(w+1)\cos L + f_m] & -\frac{g_m}{w}\chi \\ -\cos L & (w+1)\sin L + g_m & \frac{f_m}{w}\chi \\ 0 & 0 & \frac{s^2 \cos L}{2w} \\ 0 & 0 & \frac{s^2 \sin L}{2w} \\ 0 & 0 & \chi \end{bmatrix}, \tag{4}$$

where μ is the Earth gravitational parameter, $\chi = h_m \sin L - k_m \cos L$, $w = 1 + f_m \cos L + g_m \sin L$, $s = 1 + h_m^2 + k_m^2$ and the vector \mathbf{b} is:

$$\mathbf{b} = \left[0 \ 0 \ 0 \ 0 \ 0 \ \sqrt{\mu p} \left(\frac{w}{p} \right)^2 \right]^T. \tag{5}$$

The vector \mathbf{p} includes the non-Keplerian accelerations in the *radial-circumferential-angular momentum direction* frame defined in [14]. The acceleration includes disturbances (\mathbf{p}_{dist}) and the acceleration produced by the thruster (\mathbf{u}). The perturbations that can be considered, range from gravitational harmonics effects up to atmospheric drag. The mass variation due to propellant depletion is described by:

$$\dot{m}(t) = -\frac{T(t)}{c(t)}, \tag{6}$$

where m is the mass, T the thrust force magnitude, and c is the effective exhaust velocity, related to the specific impulse through $c = I_{sp}g_0$, with g_0 being the gravitational acceleration at sea level. The full state vector is then:

$$\mathbf{x} = [\mathbf{x}_m \ m]^T. \tag{7}$$

$\dot{\mathbf{x}}(t)$ is integrated numerically using a fixed-step explicit Runge-Kutta method of the 8th order.

2.2 Variable performance optimization

The methodology relates the set-point selection of the thruster to a function describing the maneuvering efficiency along the orbit [7]. A multi-objective genetic algorithm selects the parameters, optimizing the objectives. The methodology is applied to a realistic electrospray model.

2.2.1 Electro spray model

The electro spray technology relies on the extraction and acceleration of ions or droplets from a conductive liquid. Ionic liquids are composed of chemically stable mixtures of positive and negative molecular ions. The application of a difference of potential (V_e) between the liquid and an extractor grid allows for extracting and accelerating the ions at once. Being the particles already in ionic state, no ionization is required: this contributes to the high efficiencies achievable by these systems. Additionally, the emission is nearly instantaneous upon voltage application, meaning that no significant transients are observed and operations are simpler, compared to other electric propulsion technologies.

Figure 1 shows the experimental measurements carried out in IENAI SPACE's laboratories on an electro spray prototype, particularly the thrust-to-power ratio (left) and specific impulse (right) for different voltage (V_e). The system tested is composed of a thruster head (the component containing emitter and grids and producing thrust), a propellant management unit, and a power processing unit. At the lower bound (1000 V), the emission is mainly characterized by droplets in terms of mass fraction. This explains the thrust-to-power ratio and lower specific impulse, which depends on the voltage too, which is lower in this case. At the upper bound (1600 V), on the other hand, most of the extracted particles are ions, which are lighter compared to droplets. This explains the lower thrust-to-power ratio and, combined with the higher voltage, the higher specific impulse.

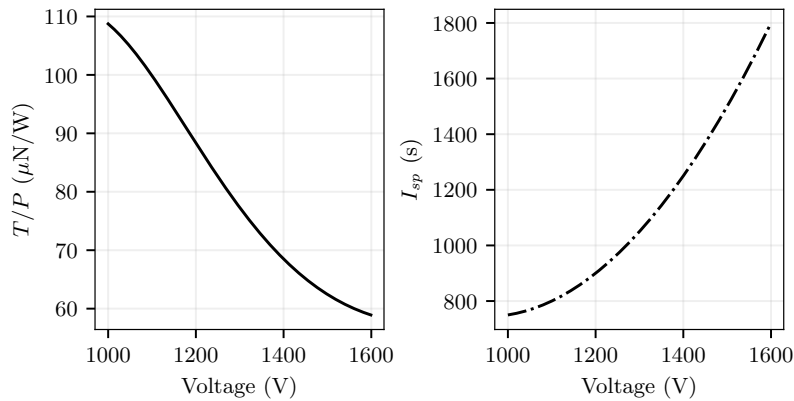


Figure 1: Thrust-to-power ratio (left), and specific impulse (right) versus emitter voltage.

These two extremes are respectively named "droplet" and "ionic" regimes in this work. We point out that the naming indicates a prevalence of one particle in terms of mass fraction, but a small portion of the remaining species is found in the beam as well. The selection of V_e and the number of active thruster heads allows one to switch between the two regimes and trade between a high-thrust performance and a high-specific impulse one while controlling the power level as well. In general, the thrust magnitude (T) for the system can be written as a function of the specific impulse (I_{sp}), the system efficiency ($\hat{\eta}$), and the input power (P_{in}):

$$T(t, I_{sp}) = \frac{2\hat{\eta}(I_{sp}(t))P_{in}}{g_0} \frac{1}{I_{sp}(t)}. \quad (8)$$

We note that the propulsion system efficiency ($\hat{\eta}$) is a function of the specific impulse. Table 1 collects relevant info on the settings to obtain each regime and the performance attainable.

2.3 Control direction selection

This work employs a Predefined Control Law (PCL) strategy to obtain near-optimal thrust direction at integration run-time, through trajectory parameterization. The PCL adopted is a Lyapunov-candidate function (V) of the form:

VARIABLE-PERFORMANCE MANEUVERS OPTIMIZATION

Table 1: Electrospray regimes.

Regime	V_e (V)	$\hat{\eta}$ (-)	T/P ($\mu N/W$)	I_{sp} (s)
Droplet	1000.0	0.40	108.7	750
Ionic	1600.0	0.52	58.9	1800

$$V(\hat{\mathbf{x}}_c) = \frac{1}{2} \hat{\mathbf{x}}_c^T \hat{\mathbf{x}}_c, \quad (9)$$

where $\mathbf{x}_c = [p, f_m, g_m, h_m, k_m]^T$ is a subset of Eq. (3) and $\hat{\mathbf{x}}_c(t) = \mathbf{x}_c(t) - \mathbf{x}_c^{(t)}$ represents the distance from the target elements $\mathbf{x}_c^{(t)}$. V is positive semi-definite, and its time derivative (\dot{V}) is:

$$\dot{V}(\hat{\mathbf{x}}_c) = \hat{\mathbf{x}}_c^T \dot{\hat{\mathbf{x}}}_c = \hat{\mathbf{x}}_c^T A(\hat{\mathbf{x}}_c) \mathbf{p}. \quad (10)$$

Note that \mathbf{b} cancels out in Eq. (10), since \mathbf{x}_c does not contain L . The controls direction ($\hat{\mathbf{u}}$) is chosen to ensure that $\dot{V}(\hat{\mathbf{x}}_c)$ is negative semi-definite:

$$\hat{\mathbf{u}} = -\frac{A(\hat{\mathbf{x}}_c)^T K \hat{\mathbf{x}}_c}{\|A(\hat{\mathbf{x}}_c)^T K \hat{\mathbf{x}}_c\|}, \quad (11)$$

where K is a positive definite matrix. This work employs a specific formulation derived by [15] targeting only semi-major axis (a), eccentricity (e), and inclination (i), since, in the presence of the J_2 perturbation and using EP, the other orbital elements are best targeted indirectly using a combination of these three, as shown in [5]. The Lyapunov function defined by [15] is called proximity quotient Q , and the reduced form used is written as:

$$Q = W_a S_a \left(\frac{a - a_t}{\dot{a}_{xx}} \right)^2 + W_e \left(\frac{e - e_t}{\dot{e}_{xx}} \right)^2 + W_i \left(\frac{i - i_t}{\dot{i}_{xx}} \right)^2, \quad (12)$$

where S_a is a scaling function preventing non-convergence in some instances and W_a , W_e , W_i are scalar weights expressing how aggressively one orbital element is targeted compared to the others [15]. \dot{a}_{xx} , \dot{e}_{xx} , and \dot{i}_{xx} are the maximum rate of change of each element over thrust direction and true anomaly, and the subscript "t" indicates the target elements.

2.3.1 Set-point selection

The variable-performance methodology developed in [7], which is suitable for continuously varying systems, relates the instantaneous thruster setpoint to a term describing the effectiveness of thrusting in a given point of the orbit. This instantaneous "effectiveness", referred to as maneuvering efficiency (η) or thrust effectivity, can be computed for a generic orbital element (z) subject to a change of Δz , as the ratio of the maximum rate of change over thrust direction and its maximum over the true anomaly:

$$\eta_{\Delta z} = \frac{\dot{z}_x}{\dot{z}_x|_{\theta_{max}}}, \quad (13)$$

If a multi-element maneuver is performed, it is possible to blend the single-element efficiencies into a single parameter, as in [15], which can be expressed as a function of the rate of the proximity quotient from Eq. (12):

$$\eta = \frac{\dot{Q}_n - \dot{Q}_{nm}}{\dot{Q}_{nx} - \dot{Q}_{nm}}, \quad (14)$$

where \dot{Q}_n is the instantaneous most negative rate of Q obtained by selecting the thrust direction according to Eq. (11), and \dot{Q}_{nm} and \dot{Q}_{nx} are respectively its minimum and maximum along the true anomaly over one orbital period. Since this work considers a discrete-state system, the selection of the set-point can be simplified to the definition of two parameters, although the philosophy of tying the selection to maneuvering efficiency from [7] is maintained. The first parameter is a coasting threshold (η_t): if the computed maneuvering efficiency is below η_t , the thruster is shut down, otherwise, it produces thrust according to the second parameter. The second parameter is a switching threshold (η_s): if the computed maneuvering efficiency is above this value the droplet mode is used, otherwise, the ionic one is activated.

Figure 2 synthesizes the regime-selection logic, showing the three modes versus the maneuvering efficiency for a given combination of coasting η_t and switching η_s thresholds, in this case respectively 0.2 and 0.7.

Thanks to this formulation, the optimization problem is translated into the selection of the combination of thresholds that minimizes the objectives. The solver used is the multi-objective genetic algorithm NSGA-2 [4]. Alongside

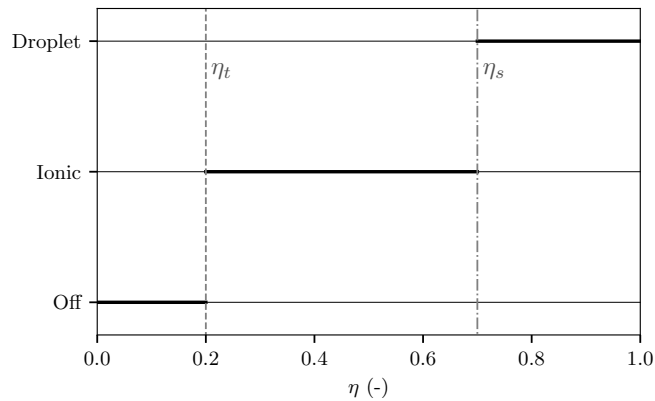


Figure 2: Regime versus maneuvering efficiency (η). Coasting (η_t) and switching (η_s) thresholds are shown as well.

the two thresholds, the genetic algorithm solves for the ratio of the weights of the predefined control law as well, since it leads to improved maneuver performance. Finally, the following design variable vector \mathbf{d} is used by the genetic algorithm:

$$\mathbf{d} = [W_e/W_a, W_i/W_a, \eta_t, \eta_s] \quad (15)$$

3. Numerical Example and Results

The numerical example considers a 5-kg CubeSat equipped with an electrospray propulsion system characterized by the performance described in Subsection 2.2.1, and with a power consumption below 10W. The system can operate in the modes (or regimes) described in Table 1. The example considers the initial and final orbital elements, as presented in Table 2, which constitute a multi-element variation maneuver. This transfer could be representative of a commission maneuver for a small satellite constellation, as shown in [6], which could be used to transfer some of the propulsive ΔV need from the launcher to the satellite, with consequent launch cost savings.

Table 2: Test case mission parameters.

Orbit	a (km)	e (-)	i ($^\circ$)
Initial	7071.0	0.01	97.77
Target	7103.0	0.0055	97.815

Figure 3 shows the Pareto optimal front of propellant mass (m_p) versus maneuver duration (t_f) for three different cases. In general, longer maneuvers are associated with a higher frequency of coasting arcs, which relates to propellant savings as well, thanks to the better exploitation of the dynamics.

In particular, for each case, the dash-dot line represents a constant droplet regime case, which has the highest thrust, but lowest specific impulse. In fact, the minimum time maneuver is below 4 days, while the propellant needed is above 20 g. On the other hand, the solid line shows the ionic regime case, which is slower but more fuel efficient. In this case, the minimum time solution is above 7.4 days, but the propellant need is more than halved, compared to the droplet mode. Note that the constant-performance cases are a subset of the optimization problem described in Eq. (1), in which the design vector Eq. (15) considers only the first three elements.

Finally, the dashed line represents the mixed case, namely the variable-performance solutions. These appear to be a compromise between the two constant-performance curves, converging to these at the minimum-time and minimum-propellant points.

VARIABLE-PERFORMANCE MANEUVERS OPTIMIZATION

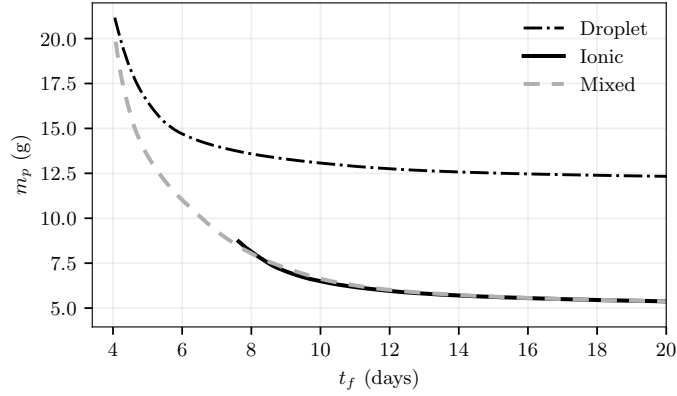


Figure 3: Pareto front of propellant mass (m_p) versus maneuver duration (t_f) for ionic, droplet, and mixed regimes.

The region of interest for variable performance is in the 4-8 day range, in which the dynamically varying mixed regime allows to perform maneuvers as fast as the droplet mode, but with less propellant. Figure 4 shows the relative difference of the variable performance against the constant cases. The comparison with the ionic mode (dashed line) reveals that no relevant improvement can be achieved since the two become equivalent. On the other hand, the mixed mode reaches up to 100% speed-ups and more than 70% propellant savings in some points, compared to the droplet regime. Notice that for large t_f , the propellant saving reaches 125%. However, in that region, it is possible to switch to the constant ionic case, which is ultimately equivalent.

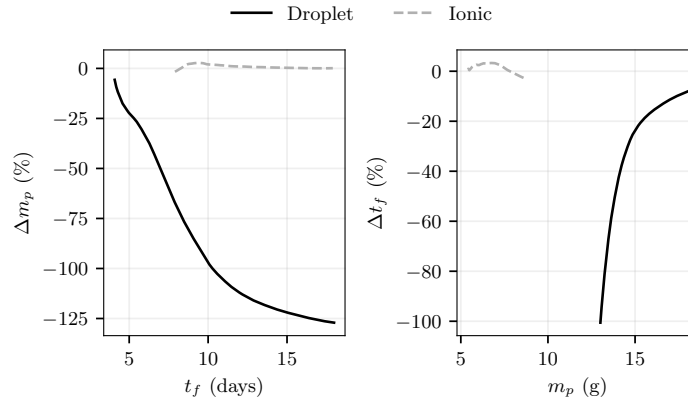


Figure 4: Mixed mode propellant saving (Δm_p) versus t_f (left) and time improvement (Δt_f) versus m_p (right), against both droplet and ionic.

The optimal maneuvering efficiency thresholds for different maneuver duration are shown in Figure 5, with matching line style with Figure 3 for each case. It is noticeable that, as the maneuver duration increases, the coasting threshold (η_t) rises as well for all the cases. This means that more coasting arcs are employed, as mentioned previously. The figure shows the switching threshold (η_s) for the mixed regime as well. The plot illustrates that the regime goes from full droplet at the minimum time to full ionic within the region of interest, explaining the convergence to the two constant cases. This can be seen from the coasting threshold as well (dashed line), which converges to the ionic one (solid line) above 9 days.

Figure 6 reports the optimal weights ratios for different t_f , showing similar profiles for all the cases. Both the W_e/W_a and W_i/W_a ratios start at around 2 for the minimum time solutions and grow up to 6 for the longer transfers, although the mixed case exhibits a slightly different profile.

The region of interest is further analyzed to improve the understanding and implications of the use of a variable-performance approach. Particularly, four sample solutions from the Pareto front of Figure 3 are selected, corresponding to the solutions with a final time of respectively 3.95, 4.85, 5.88, and 8.14 days.

Figure 7 shows the evolution of semi-major axis (top), orbital average thrust (middle), and orbital average specific impulse (bottom) over time (t). The semi-major axis plot shows the convergence from the initial to the target for each

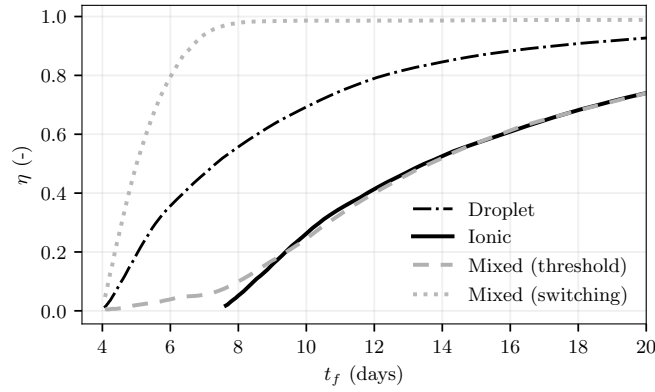


Figure 5: Maneuvering efficiency threshold (η_t and η_s) versus maneuver duration (t_f).

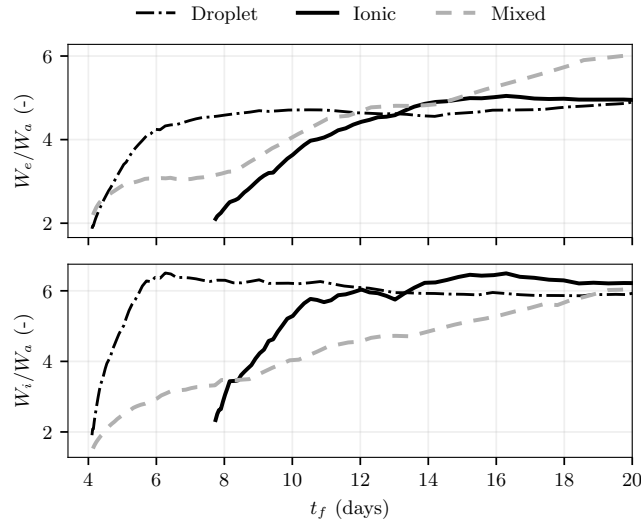


Figure 6: Optimal weights ratios versus t_f for droplet, ionic, and mixed regimes.

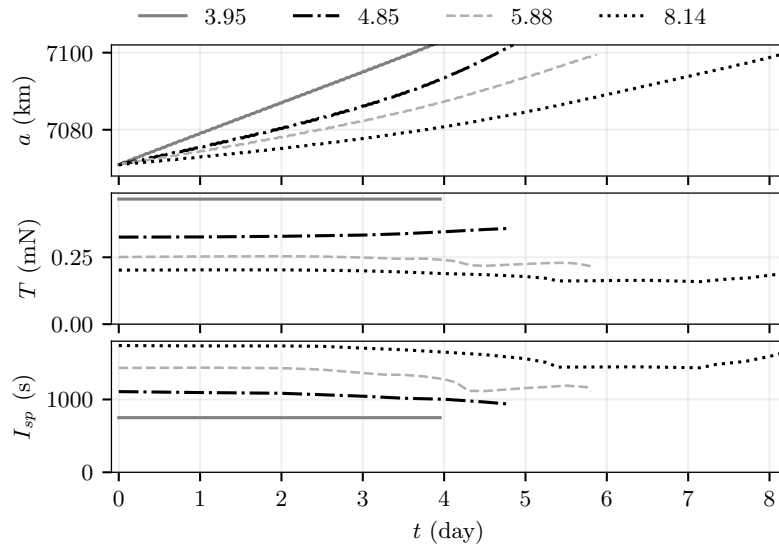
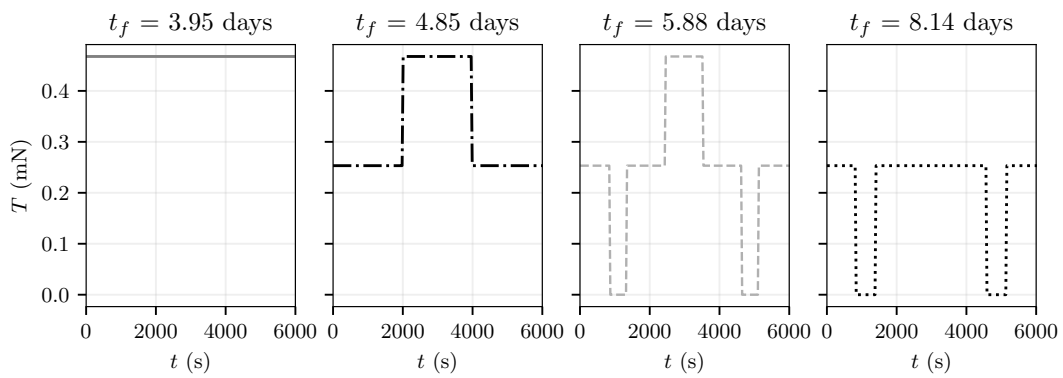
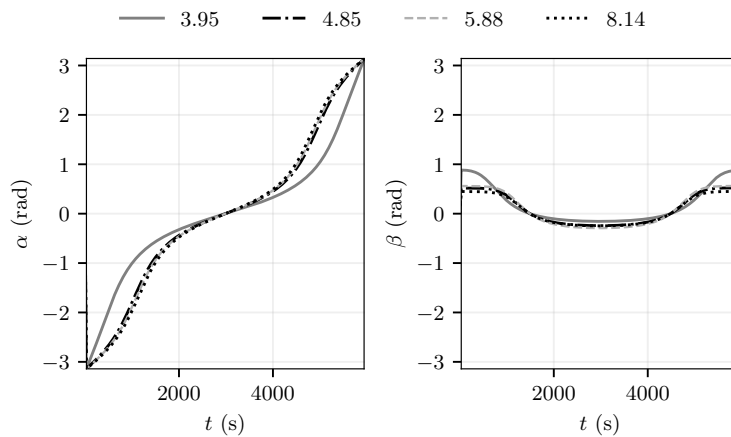
solution. Similar curves are found for the other targeted elements, not shown for conciseness. The orbital average thrust and specific impulse, on the other hand, highlight that the mixed regime enables two things: first, even though the system has only two discrete states, intermediate average values are reached by tuning the switching. Second, the average is not constant over time, in line with [10].

Figure 8 illustrates the thrust profile over the first revolution for the four solutions highlighted. The fastest solution (3.95 days) employs a continuous maximum thrust burn, namely, it is always in a full droplet regime. As the maneuver duration is increased (4.85 days), the optimal solution still requires continuous firing, but switching between the two regimes is needed, with an approximate subdivision of 33% for the droplet regime and 66% for the ionic one. As the duration gets longer (5.88 days), coasting arcs begin to appear, and the ionic regime is the predominant one, with the droplet being used only in a small portion of the orbit, where a higher thrust is more convenient. Finally, at 8.14 days of duration, the droplet regime disappears, leaving a discontinuous full ionic regime, with coasting arcs growing in span.

Finally, the thrusting angle profiles over the first revolution are shown in Figure 9. The plot on the left shows the in-plane angle (α) and the one on the right displays the out-of-plane angle (β), as defined by [15]. The minimum-time solution (3.95 days) exhibits a different attitude profile compared to the other solutions analyzed, with larger out-of-plane angles, meaning that the inclination is being targeted more aggressively at the beginning, while the other cases are more homogeneous.

Practically, to carry out the maneuver's operation, the satellite would require both the desired attitude from Figure 9 and the mode selection profile from Figure 8, which could be interpolated over time or true anomaly, depending on the navigation sensors onboard. A constant-performance case would require only the attitude, meaning that the

VARIABLE-PERFORMANCE MANEUVERS OPTIMIZATION

Figure 7: Semi-major axis, average thrust, and I_{sp} profiles for $t_f = [3.95, 4.85, 5.88, 8.14]$ days.Figure 8: Thrust over the first revolution for $t_f = [3.95, 4.85, 5.88, 8.14]$ days.Figure 9: In-plane (left) and out-of-plane (right) angles over first orbit for $t_f = [3.95, 4.85, 5.88, 8.14]$ days.

increase in operational complexity, if variable performance is enabled, is minor.

4. Conclusion

This work presents the application of a variable performance optimization methodology to an electrospray thruster model, intending to improve the performance of small satellites' maneuvers. The study is motivated by the capability of electrospray propulsion to operate in various emission regimes, which can be employed for better exploitation of the propulsion system throughout the maneuver. The optimization methodology employs a candidate-Lyapunov function to compute the thrusting angles. A maneuvering efficiency parameter is used to describe the effectiveness of thrusting at a given point in the orbit, and a coasting and a switching threshold are defined to select the operating modes, as a function of the maneuvering efficiency. A multi-objective genetic algorithm tunes the candidate-Lyapunov function weights while selecting the optimal coasting and switching thresholds, optimizing propellant mass and maneuver duration in the same iteration, and generating Pareto optimal fronts that could be used for mission design and system trade studies. The numerical example presented shows that a real-time dynamic switching between the two operational regimes enables improved maneuver performance. The improvement is concentrated in a region of interest between the two constant-performance cases, where the variable-performance case outperforms the droplet mode by up to 100% in terms of maneuvering time and more than 70 % in propellant usage. A practical implementation of this discrete variable performance maneuver would require only a minor increase in operational complexity, making this capability of great interest for enhancing the performance of small satellites.

5. Acknowledgments

This project has received funding from the “Comunidad de Madrid” under “Ayudas destinadas a la realización de doctorados industriales” program IND2020/TIC-17317.

References

- [1] Lorenzo Casalino and Guido Colasurdo. Optimization of Variable-Specific-Impulse Interplanetary Trajectories. *Journal of Guidance, Control, and Dynamics*, 27(4):678–684, July 2004.
- [2] Zhemin Chi, Di Wu, Fanghua Jiang, and Junfeng Li. Optimization of Variable-Specific-Impulse Gravity-Assist Trajectories. *Journal of Spacecraft and Rockets*, 57(2):291–299, March 2020.
- [3] Edgar Y. Choueiri. A Critical History of Electric Propulsion: The First 50 Years (1906-1956). *Journal of Propulsion and Power*, 20(2):193–203, March 2004. Publisher: American Institute of Aeronautics and Astronautics.
- [4] Kalyanmoy Deb, Amrit Pratap, Sameer Agarwal, and T. Meyarivan. A fast and elitist multiobjective genetic algorithm: NSGA-II. *IEEE Transactions on Evolutionary Computation*, 6(2):182–197, April 2002. Conference Name: IEEE Transactions on Evolutionary Computation.
- [5] Giuseppe Di Pasquale, Manuel Sanjurjo Rivo, and Daniel Pérez Grande. Optimal Low-Thrust Orbital Plane Spacing Maneuver for Constellation Deployment and Reconfiguration including J_2 . In *AIAA SCITECH 2022 Forum*, San Diego, CA & Virtual, January 2022. American Institute of Aeronautics and Astronautics.
- [6] Giuseppe Di Pasquale, Manuel Sanjurjo-Rivo, and Daniel Pérez Grande. Optimization of constellation deployment using on-board propulsion and Earth nodal regression. *Advances in Space Research*, 70(11):3281–3300, December 2022.
- [7] Giuseppe Di Pasquale, Manuel Sanjurjo Rivo, and Daniel Pérez Grande. A Novel Variable Specific Impulse Optimization Methodology for Modulable Electric Propulsion Systems. In *AIAA SCITECH 2023 Forum*, AIAA SciTech Forum. American Institute of Aeronautics and Astronautics, January 2023.
- [8] Giancarlo Genta and P. Federica Maffione. Optimal low-thrust trajectories for nuclear and solar electric propulsion. *Acta Astronautica*, 118:251–261, January 2016.
- [9] Jean Albert Kechichian. Optimal low-thrust transfer using variable bounded thrust. *Acta Astronautica*, 36(7):357–365, October 1995.
- [10] Craig A. Kluever. Geostationary Orbit Transfers Using Solar Electric Propulsion with Specific Impulse Modulation. *Journal of Spacecraft and Rockets*, 41(3):461–466, May 2004.

VARIABLE-PERFORMANCE MANEUVERS OPTIMIZATION

- [11] Giovanni Mengali and Alessandro A. Quarta. Fuel-Optimal, Power-Limited Rendezvous with Variable Thruster Efficiency. *Journal of Guidance, Control, and Dynamics*, 28(6):1194–1199, November 2005. Publisher: American Institute of Aeronautics and Astronautics.
- [12] Steven Oleson. Mission advantages of constant power, variable Isp electrostatic thrusters. In *36th AIAA/ASME/SAE/ASEE Joint Propulsion Conference and Exhibit*, Las Vegas, NV, U.S.A., July 2000. American Institute of Aeronautics and Astronautics.
- [13] Dillon O'Reilly, Georg Herdrich, and Darren F. Kavanagh. Electric Propulsion Methods for Small Satellites: A Review. *Aerospace*, 8(1):22, January 2021. Number: 1 Publisher: Multidisciplinary Digital Publishing Institute.
- [14] Anastassios E. Petropoulos. Simple control laws for low-thrust orbit transfers. In *AAS/AIAA Astrodynamics Specialists Conference*, 2003.
- [15] Anastassios E. Petropoulos. Refinements to the Q-law for the low-thrust orbit transfers. In *15th AAS/AIAA Space Flight Mechanics Conference, Copper Mountain, CO, January 23-27, 2005*, January 2005. Accepted: 2005-09-15T22:20:16Z Publisher: Pasadena, CA : Jet Propulsion Laboratory, National Aeronautics and Space Administration, 2005.
- [16] Madeleine Schroeder, Amelia Bruno, and Paulo C. Lozano. Ionic Liquid Electrospray Transient Emission Characterization. In *AIAA SCITECH 2022 Forum*, AIAA SciTech Forum. American Institute of Aeronautics and Astronautics, December 2021.
- [17] Hans Seywald, Carlos M. Roithmayr, Patrick A. Troutman, and Sang-Young Park. Fuel-Optimal Transfers Between Coplanar Circular Orbits Using Variable-Specific-Impulse Engines. *Journal of Guidance, Control, and Dynamics*, 2005.
- [18] David Villegas, Sara Correyero, Mick Wijnen, and Pablo Fajardo. Indirect Characterization of ATHENA Performance, a Novel Externally Wetted Electrospray Propulsion System. In *Space Propulsion Conference 2022*, 2022.